

REPEATABILITY AND LONGITUDINAL ASSESSMENT OF FOVEAL CONE STRUCTURE IN *CNGB3*-ASSOCIATED ACHROMATOPSIA

CHRISTOPHER S. LANGLO, PhD,* LAURA R. ERKER, PhD,† MARIA PARKER, MD,† EMILY J. PATTERSON, PhD,‡ BRIAN P. HIGGINS, BS,‡ PHYLLIS SUMMERFELT, BA,‡ MOATAZ M. RAZEEN, MD,‡§ FREDERICK T. COLLISON, OD,¶ GERALD A. FISHMAN, MD,¶ CHRISTINE N. KAY, MD,** JING ZHANG, MD,** RICHARD G. WELEBER, MD,† PAUL YANG, MD, PhD,† MARK E. PENNESI, MD, PhD,† BYRON L. LAM, MD,†† JEFFREY D. CHULAY, MD,‡‡ ALFREDO DUBRA, PhD,*‡§§ WILLIAM W. HAUSWIRTH, PhD,¶¶ DAVID J. WILSON, MD,† JOSEPH CARROLL, PhD*‡§§ FOR THE ACHM-001 STUDY GROUP

Purpose: Congenital achromatopsia is an autosomal recessive disease causing substantial reduction or complete absence of cone function. Although believed to be a relatively stationary disorder, questions remain regarding the stability of cone structure over time. In this study, the authors sought to assess the repeatability of and examine longitudinal changes in measurements of central cone structure in patients with achromatopsia.

Methods: Forty-one subjects with *CNGB3*-associated achromatopsia were imaged over a period of between 6 and 26 months using optical coherence tomography and adaptive optics scanning light ophthalmoscopy. Outer nuclear layer (ONL) thickness, ellipsoid zone (EZ) disruption, and peak foveal cone density were assessed.

Results: ONL thickness increased slightly compared with baseline (0.184 $\mu\text{m}/\text{month}$, $P = 0.02$). The EZ grade remained unchanged for 34/41 subjects. Peak foveal cone density did not significantly change over time (mean change 1% per 6 months, $P = 0.126$).

Conclusion: Foveal cone structure showed little or no change in this group of subjects with *CNGB3*-associated achromatopsia. Over the time scales investigated (6–26 months), achromatopsia seems to be a structurally stable condition, although longer-term follow-up is needed. These data will be useful in assessing foveal cone structure after therapeutic intervention.

RETINA 37:1956–1966, 2017

Achromatopsia is a congenital retinal disease associated with substantially reduced or absent cone function. With the exception of the recent link to *ATF6*,¹ achromatopsia is caused by mutations in genes encoding components of the cone phototransduction cascade (*CNGA3*, *CNGB3*, *GNAT2*, *PDE6C*, and *PDE6H*).^{2–6} Despite this functional deficit, imaging studies using optical coherence tomography (OCT) demonstrate a well-defined outer nuclear layer (ONL) at the fovea in the majority of cases.^{7–10} Moreover, the appearance of the ellipsoid zone (EZ), which is also called the inner and outer segment junction (IS/OS), and the interdigitation

zone (IZ) can be nearly normal (contiguous) in appearance, although some level of disruption is more typical.^{7,9–11} Additionally, studies using reflectance-based adaptive optics (AO) imaging have demonstrated nonreflective regions at the fovea and variable numbers of non-waveguiding cones in the parafovea,^{12,13} and there is some evidence for genotype-dependent differences in the appearance of the cone mosaic.¹⁴ More recently, split-detection AO scanning light ophthalmoscopy (AOSLO) has provided direct evidence for remnant cone inner segments at the fovea of patients with *CNGB3*-associated achromatopsia, with peak

density ranging from about 7,000 to about 53,000 cones/mm²—though these values are all well below normal peak cone density of around 85,000 to 324,000 cones/mm².^{15–18} Considering emerging

From the *Department of Cell Biology, Neurobiology and Anatomy, Medical College of Wisconsin, Milwaukee, Wisconsin; †Casey Eye Institute, Oregon Health & Science University, Portland, Oregon; ‡Department of Ophthalmology, Medical College of Wisconsin, Milwaukee, Wisconsin; §Alexandria Faculty of Medicine, University of Alexandria, Alexandria, Egypt; ¶Pangere Center for Inherited Retinal Diseases, The Chicago Lighthouse, Chicago, Illinois; **Vitreo Retinal Associates, Gainesville, Florida; ††Bascom Palmer Eye Institute, University of Miami, Miami, Florida; ‡‡Applied Genetics Technologies Corporation (AGTC), Alachua, Florida; §§Department of Biophysics, Medical College of Wisconsin, Milwaukee, Wisconsin; and ¶¶Department of Ophthalmology, University of Florida, Gainesville, Florida.

Supported in part by the National Center for Research Resources and the National Center for Advancing Translational Sciences of the National Institutes of Health (NIH) under award number UL1TR000055, by the National Eye Institute of the NIH under award numbers R01EY017607, P30EY001931, P30EY021721, P30EY010572 (OHSU), R24EY022023, U01EY025477, K08EY021186 (M.E.P.), K08EY026650, and T32EY014537, and by the National Institute of General Medical Sciences of the NIH under award number T32GM080202. The content is solely the responsibility of the authors and does not necessarily represent the official views of the NIH. Additional support was provided by Foundation Fighting Blindness under award numbers CDNMT07140648OHSU (P.Y.), CDNMT09140659OHSU (M.E.P.), CCL07110534OHSU01 (CEJ), Unrestricted departmental support from Research to Prevent Blindness, Macula Vision Research Foundation, AGTC, C.M. Overstreet Retinal Eye Disease Research Fund, AchromaCorp and the Pangere Family Foundation. This investigation was conducted in part in a facility constructed with support from a Research Facilities Improvement Program, Grant number C06RR016511 from the National Center for Research Resources, NIH.

C. S. Langlo has received an honorarium and travel reimbursement from AGTC. G. A. Fishman receives research support from AGTC and is a consultant for Spark. C. N. Kay receives research support from Foundation Fighting Blindness and AGTC and is a consultant for AGTC and Second Sight. R. G. Weleber receives research support from AGTC, Sanofi, and Foundation Fighting Blindness and serves on the advisory boards for AGTC and Foundation Fighting Blindness. P. Yang receives research support from AGTC. M. E. Pennesi receives research support from AGTC and Sanofi and is a consultant for Spark, Editas, ProQR Therapeutics, Ionis Pharmaceuticals, and AGTC. B. L. Lam receives research support from AGTC and Ocata and is a consultant for AGTC, Spark, Shire, and Ionis Pharmaceutical. J. D. Chulay is an employee of and holds shares in AGTC. A. Dubra is a consultant for Meira GTx, and holds a related US Patent (8,226,236). W. W. Hauswirth, receives research support from, is a consultant for, and holds shares of AGTC. D. J. Wilson receives research support from AGTC. J. Carroll receives research support from AGTC and OptoVue and is a consultant for Meira GTx. The remaining authors have no financial/conflicting interests to disclose.

W. W. Hauswirth and the University of Florida have a financial interest in the use of AAV therapies, and own equity in a company (AGTC) that might, in the future, commercialize some aspects of this work. R. G. Weleber serves on advisory boards for AGTC and Foundation Fighting Blindness; these relationships have been reviewed and managed by OHSU.

This is an open-access article distributed under the terms of the Creative Commons Attribution-Non Commercial-No Derivatives License 4.0 (CCBY-NC-ND), where it is permissible to download and share the work provided it is properly cited. The work cannot be changed in any way or used commercially without permission from the journal.

Reprint requests: Joseph Carroll, PhD, Department of Ophthalmology, Medical College of Wisconsin, 925 North 87th Street, Milwaukee, WI 53226-0509; e-mail: jcarroll@mcw.edu

gene therapy trials, this variability in remnant cone structure could serve as an important predictor of therapeutic potential across patients. Also essential to the success of these trials will be defining the expected rate of central cone loss in achromatopsia.

Achromatopsia is generally believed to be a relatively stationary condition—symptoms including reduced visual acuity, photoaversion, and impaired color discrimination are all stable throughout life, although nystagmus tends to decrease with age.^{19,20} In contrast, there are conflicting reports regarding the stability of retinal structure over the lifespan of individual subjects. Thomas et al¹⁰ reported that there was progression over a follow-up period of 11 months to 25 months with greater disruption of the EZ (IS/OS) band on OCT, and thinning of the retina in younger patients; ONL thickness was stable in older patients. Aboshiha et al⁸ found no qualitative change in the EZ (IS/OS) band in 35 of 37 subjects, and no statistically significant change in ONL thickness in the 34 subjects in which the ONL could be measured, over a mean follow-up of 19.5 months. Cross-sectional studies have also reported conflicting results. Within a population of 40 genetically confirmed subjects examined with OCT imaging, Sundaram et al⁷ found no age dependence for the degree of photoreceptor layer disruption or ONL thinning. In contrast, Langlo et al¹⁶ showed greater photoreceptor layer disruption in older subjects, but found no relationship between ONL thickness and age within a population of 51 subjects with *CNGB3*-associated achromatopsia. Thiadens et al⁹ also reported a strong age association with loss of the EZ (IS/OS) band on OCT examination of 40 subjects, and Thomas et al¹⁰ showed EZ (IS/OS) disruption primarily in older subjects and a linear correlation between age and ONL thickness in 13 subjects. Indeed, Yang et al²¹ reported that in early childhood, the spectrum of foveal pathology on OCT examination in 9 subjects, between 1 and 8 years of age, was generally milder than that of previously published studies on older subjects, but that neither age alone nor genotype alone predicts the degree of photoreceptor loss or preservation. Among the challenges in comparing these studies were the different periods over which measurements were made and the variable genetic makeup of the study populations.

An additional limitation of these OCT studies is that conventional OCT systems lack the transverse resolution to observe individual cone cells; thus there may be changes that are not detectable with OCT. In contrast, AOSLO provides greater lateral resolution, revealing the photoreceptor mosaic,^{22,23} and has been shown in many cases to detect photoreceptor disruption that was not visible on OCT.^{24,25} Moreover, AOSLO has been

used to monitor cone structure over time with high sensitivity as demonstrated in individuals with retinitis pigmentosa.²⁶ In addition, in patients with cone mosaic disturbances, locations previously devoid of reflective cone structure were shown to regenerate a reflective confocal signal.^{27,28} Here we present the first longitudinal study of foveal cone density in patients with *CNGB3*-associated achromatopsia.

Methods

Subjects

This research followed the tenets of the Declaration of Helsinki and was approved by the Institutional Review Boards at the Medical College of Wisconsin, Oregon Health & Science University (OHSU), University of Florida, University of Miami, and Western Institutional Review Board. Forty-one subjects with genetically confirmed biallelic mutations in *CNGB3* were recruited through one of four sites (Bascom Palmer Eye Institute, Miami, FL; OHSU Casey Eye Institute, Portland, OR; The Chicago Lighthouse, Chicago, IL; and Vitreo Retinal Associates, Gainesville, FL) as part of a natural history study (clinicaltrials.gov identifier NCT02599922) in which a clinical examination and visual acuity assessment were performed. Genetic characterization of these subjects was previously reported.¹⁶ High-resolution ophthalmic imaging was performed at the Medical College of Wisconsin for both eyes, and the eye with the better image quality was chosen for subsequent analysis. Subjects returned for 2 to 4 follow-up visits between November 2013 and September 2015, with intervisit spacing between 4 and 12 months (mean = 6.6).

Optical Coherence Tomography

Dilation was induced with one drop of tropicamide (1%) and one drop of phenylephrine hydrochloride (2.5%) in each eye before imaging. All subjects underwent examination with Bioptigen SD-OCT (Bioptigen, Morrisville, NC). Vertical and horizontal line scans centered on the fovea (7 mm nominal scan length, 1,000 A-scans/B-scan, 120 B-scans) and vertical and horizontal macular volume scans (7 × 7 mm nominal scan length, 750 A-scans/B-scan, 250 B-scans) were obtained for each eye at each visit. Volume scans were used to identify the center of the foveal pit and ensure that line scans were obtained through this location. The foveal line scans were graded for each visit using the scheme defined by Sundaram et al, which describes the degree of disruption in the EZ (IS/OS) band.⁷ Briefly, Grade I corre-

sponds to an intact band, Grade II corresponds to focal disruption of the band, Grade III corresponds to an absence of the band, Grade IV describes a hyporeflective region below the external limiting membrane (ELM), and Grade V corresponds to outer retinal atrophy. Measurements of ONL thickness were then taken by measuring a 5-pixel wide longitudinal intensity profile at the foveola, as previously reported.¹⁶

Adaptive Optics Scanning Light Ophthalmoscopy

Confocal and split-detector AOSLO imaging were performed simultaneously using a previously described instrument.^{29,30} An 850-nm superluminescent diode was used for wavefront sensing, and a 790-nm superluminescent diode was used for image acquisition. Images were captured as AVI videos with both $1 \times 1^\circ$ and $1.75 \times 1.75^\circ$ fields of view, with the subject tracking an external fixation target to control the retinal area being imaged. Imaging was performed in a $5 \times 5^\circ$ grid centered at the foveola, and out to 12° radially both temporally and superiorly from the foveola, all sampled at 1° intervals.

Sinusoidal distortion is present in all images due to the scanning nature of the instrument. These distortions were mitigated during the image registration process as previously described.^{16,31} The confocal and split-detector images were captured and registered simultaneously thus ensuring a perfect alignment between these two image modalities. Registered images were montaged either manually or automatically using i2k Retina (DualAlign, Clifton Park, NY). Manual mounting entailed importing the registered images to Adobe Photoshop using custom software in MATLAB (MathWorks, Natick, MA) that allows the user to sort through the multiple images produced from each AVI and select those of the best quality (high signal to noise and minimal intraframe distortion). Images were then manually aligned with the position of confocal and split-detector images kept linked to one another, to eventually produce a two-layered montage with each layer consisting of one imaging modality. Scaling was determined by measuring the pixels per degree of the image using a ruling of known spacing and using the small angle approximation. The pixels per degree value was scaled linearly by the subject's axial length, based on a reference axial length of 24 mm, then multiplied by the retinal magnification factor of $291 \mu\text{m}/\text{degree}$ to obtain a final $\mu\text{m}/\text{pixel}$ image scale value.

Measuring Cone Density

Images acquired at baseline were previously used to calculate the value and location of the peak cone density in the rod-free region of the fovea, using

Table 1. OCT Grade and ONL Thickness Across the Follow-up Period

Subject	Baseline			Follow-up 1			Follow-up 2			Follow-up 3		
	Age, Years	OCT Grade	ONL Thickness, μm	Months	OCT Grade	ONL Thickness, μm	Months	OCT Grade	ONL Thickness, μm	Months	OCT Grade	ONL Thickness, μm
BPE-003	16	4	87.36	8	4	82.37	15	4	86.11	NV		
BPE-010	13	4	84.86	6	4	93.60	12	4	92.35	NV		
BPE-012	6	1	82.37	6	1	91.10	12	1	86.11	NV		
BPE-018	8	1	79.87	7	1	97.34	13	1	88.61	NV		
BPE-019	23	4	59.90	7	4	71.13	NV			NV		
BPE-022	31	4	67.39	6	4	61.15	NV			NV		
CEI-001	18	2	61.15	7	2	74.88	12	2	71.14	NV		
CEI-002	33	2	47.24	6	4	72.38	12	4	66.14	NV		
CEI-003	9	1	73.63	6	1	81.12	12	1	86.11	NV		
CEI-004	11	2	122.30	6	2	126.05	12	2	128.54	NV		
CEI-005	13	1	74.88	5	2	79.87	12	2	77.38	NV		
CEI-006	31	1	68.64	6	1	76.13	12	1	78.62	NV		
CEI-008	16	1	81.12	6	2	89.86	11	2	79.87	NV		
CEI-009	30	4	73.38	7	2	74.88	NV			NV		
CEI-010	16	1	73.63	5	1	82.37	12	1	77.37	NV		
CEI-011	22	1	96.10	6	1	92.35	NV			NV		
PCI-001	27	1	99.84	11	1	104.83	18	1	107.33	NV		
PCI-002	18	1	84.86	11	1	86.11	18	1	82.37	NV		
PCI-004	13	2	66.14	9	2	68.64	16	2	67.39	26	2	64.9
PCI-005	11	2	54.91	9	1	46.18	16	1	52.42	26	2	52.42
PCI-006	10	4	68.64	7	4	74.88	11	4	69.89	NV		
PCI-007	17	2	84.86	10	4	77.38	15	4	81.12	26	4	77.38
PCI-008	40	4	NQ	9	4	51.17	16	4	57.41	25	4	52.42
PCI-009	16	2	58.66	6	NQ	NQ	12	2	64.90	NV		
PCI-011	44	2	79.87	6	2	81.12	12	2	74.88	NV		
PCI-012	8	4	62.40	12	NQ	NQ	NV			NV		
PCI-013	17	4	61.15	6	4	66.14	11	4	63.65	NV		
PCI-017	35	2	61.15	6	2	47.42	11	2	59.90	NV		
PCI-020	27	2	68.64	6	2	67.39	NV			NV		
PCI-021	37	2	73.63	7	2	74.88	12	2	76.13	NV		
PCI-024	42	1	73.63	7	1	81.12	13	1	76.13	NV		
PCI-031	32	4	76.13	4	4	82.37	10	4	81.12	NV		
UFC-001	24	4	56.16	6	4	56.16	12	4	63.65	NV		
UFC-002	33	4	52.42	6	4	52.42	12	4	51.17	NV		
UFC-003	43	2	68.64	5	2	83.62	12	2	77.38	NV		
UFC-004	8	1	64.90	7	1	69.89	12	1	78.62	NV		
UFC-005	14	1	89.86	5	1	93.60	11	1	102.34	NV		
UFC-006	8	3	54.91	6	3	54.91	12	3	57.41	NV		
UFC-007	22	4	93.60	5	4	79.87	11	4	82.37	NV		
UFC-008	17	1	94.85	6	1	93.60	11	1	91.10	NV		
UFC-009	15	1	93.60	6	2	92.35	11	2	92.35	NV		

NQ, images were not quantifiable at this time point; NV, no visit for this time point.

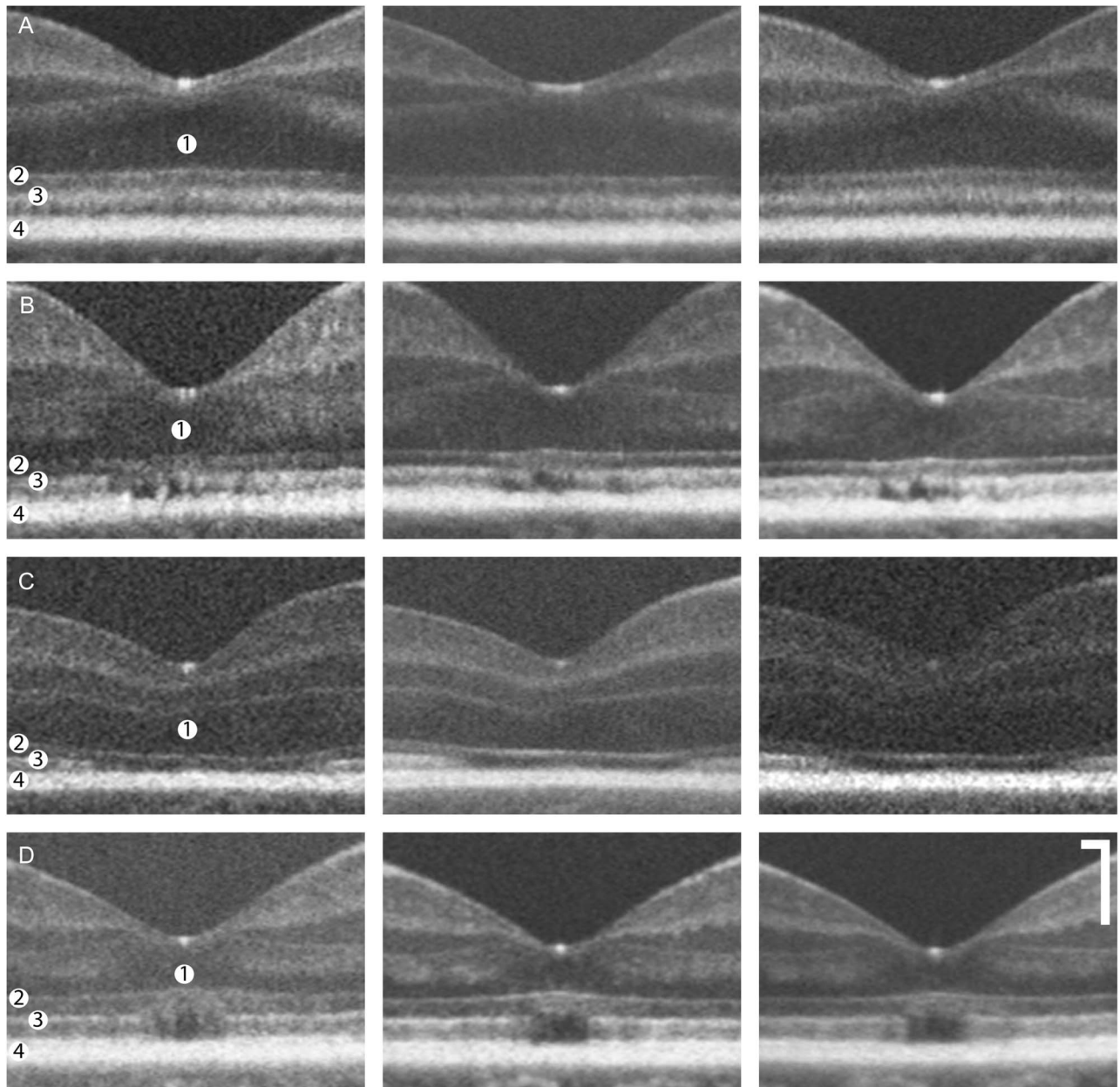


Fig. 1. Four representative examples of subjects (one of each OCT grade) whose degree of EZ (IS/OS) disruption remained unchanged across 12 months of follow-up. **A.** In subject BPE-018, there was no disruption in the EZ (IS/OS) observed across all time points. **B.** There was a small but constant amount of disruption in the retina of subject PCI-021 over 12 months. **C.** The dropout of the EZ (IS/OS) in Grade III subject UFC-006 did not seem to get wider, nor were there changes in the ELM. **D.** The hyporeflective zone in subject UFC-002 remained unchanged across the follow-up period. Scale bars = 200 μm , layers labeled as follows: 1, ONL; 2, ELM; 3, EZ (IS/OS); 4, RPE.

a $55 \times 55\text{-}\mu\text{m}$ sampling window.¹⁶ Montages from subsequent time points were then resampled to have the same pixel scale as the baseline image. The resampled follow-up montages were manually aligned to the baseline montage, and a $100 \times 100\text{-}\mu\text{m}$ region of interest was cropped from the same retinal area of both images, centered on the location of peak density. Because of differences in image distortion between imaging sessions, these two regions of interest are

not in perfect register after scaling and manual alignment. To account for these differences in distortion, the images were imported into Fiji³² and the follow-up image was warped to the baseline image using the plugin bUnwarpJ.³³ The center $55 \times 55\text{-}\mu\text{m}$ area was then cropped from this warped image, and each cone within this area was manually identified by a single observer (C.S.L.), then the density was calculated in cones/ mm^2 . This process was repeated for each

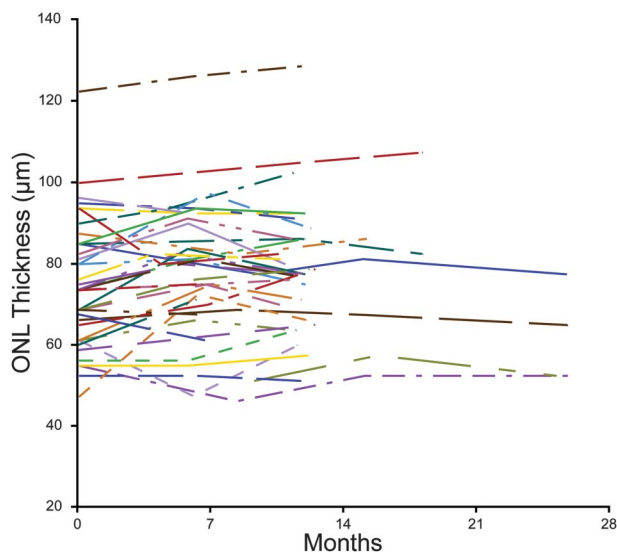


Fig. 2. ONL thickness for each subject measured throughout this study. Each line represents the ONL values for a given subject. Although there is variability in magnitude and direction of individual changes, there is an overall positive slope to these values indicating a significant increase in ONL thickness at a rate of $0.184 \mu\text{m}$ per month ($P = 0.02$).

follow-up time point (by the same observer) and compared with the baseline value.

Statistical Analysis

Repeatability of measurements was determined by calculating the intraclass correlation of triplicate measurements made by a single reviewer of the baseline ONL thickness and AOSLO cone density measurements. A random intercept linear model for the effect of time on ONL thickness was used, which accounts for each subject having their own slope and intercept. A similar random intercept linear model was used for the effect of time on cone density; cone density values were taken as the average of the three values counted by a single observer for each image. Statistical analysis was performed using SAS version 9.2 (SAS, Cary, NC).

Results

Subjects

The 41 subjects in this study were part of a larger cohort reported previously.¹⁶ The age range in these 41 subjects at baseline was from 6 years to 44 years (mean = 21.3 years). Subjects returned for follow-up imaging at intervals between 4 and 12 months (mean = 6.6 months), for a total follow-up time ranging from 6 months to 26 months (mean = 12.8 months). Including baseline imaging, the follow-up period consisted of 2 visits for 6 subjects, 3 visits for 31 subjects, and 4

visits for 3 subjects. For one subject, imaging at follow-up could not be obtained because of poor image quality.

Repeatability of Adaptive Optics Scanning Light Ophthalmoscopy and Outer Nuclear Layer Measurements

Although the repeatability of AOSLO-based measures of parafoveal cone density has been reported for normal subjects,^{34,35} the reduced image quality and disrupted photoreceptor structure in patients with achromatopsia necessitates a separate evaluation of repeatability. To assess the repeatability of the single reviewer in this study, the set of baseline AOSLO images was manually counted three times. The ONL thickness values from baseline OCT images were also measured three times. The intraclass correlation value for the cone density measurements was 0.97 (95% confidence limits 0.82–0.99) and for ONL thickness was 0.91 (95% confidence limits 0.86–0.95), indicating that these measurements were highly repeatable.

Optical Coherence Tomography Shows Slight Outer Nuclear Layer Thickening

Optical coherence tomography images were successfully acquired at each time point for 38 subjects (Table 1). In two subjects, there was one time point at which poor image quality prevented assessment of OCT images, and in one subject images were analyzed only at baseline because of poor image quality at the follow-up time point. The outer retinal grade was assessed at each time point. For seven subjects, a grade change was observed—these changes were from Grade I to II for three subjects, from Grade II to IV for two subjects, from Grade II to I for one subject, and from Grade IV to II for one subject. Although the degree of outer retinal disruption is increased for five subjects, there is a seeming decrease for two others. For the majority of subjects, there was little to no qualitative change observed in the EZ (IS/OS) band for subjects in this cohort (Figure 1). The ONL thickness varied by a mean of 2.7% between visits. The measured ONL thickness changes ranged between a $13.7\text{-}\mu\text{m}$ loss to a $25\text{-}\mu\text{m}$ gain (mean = $+1.53 \mu\text{m}$, Figure 2). Our linear model indicated that there was overall a small increase in ONL thickness of $0.184 \mu\text{m}/\text{month}$ ($P = 0.02$).

Adaptive Optics Scanning Light Ophthalmoscopy Measures of Cone Density Indicate Stability

Adaptive optics scanning light ophthalmoscopy imaging was not always successful due primarily to

Table 2. Peak Cone Density Across the Follow-up Period

Subject ID	Baseline		Follow-up 1		Follow-up 2	
	Age, Years	Density, Cones/mm ²	Months	Density, Cones/mm ²	Months	Density, Cones/mm ²
BPE-003	16	9,917	8	9,256	15	8,925
BPE-018	8	36,033	7	28,099	13	NQ
BPE-019	23	8,595	7	10,578	NV	
CEI-001	18	NQ	5	10,578	12	12,561
CEI-002	33	18,512	6	21,487	12	NQ
CEI-006	31	39,338	6	NQ	12	33,057
CEI-008	16	18,512	6	15,867	11	NQ
PCI-004	13	14,876	9	13,553	16	13,553
PCI-007	17	12,231	10	13,884	15	10,578
PCI-008	40	6,611	9	6,942	16	5,619
PCI-009	16	19,173	6	16,198	12	NQ
PCI-013	17	13,884	6	14,545	11	NQ
PCI-017	35	15,537	6	15,537	11	18,512
PCI-021	37	41,652	7	42,975	12	43,636
UFC-001	24	12,561	6	14,545	12	15,206
UFC-002	33	13,553	6	13,884	12	13,223
UFC-004	8	35,041	7	35,041	12	NQ
UFC-006	8	13,553	6	14,545	12	NQ

NQ, images were not quantifiable at this time point; NV, no visit for this time point.

nystagmus in these patients, resulting in images that could not be analyzed.¹⁶ Images for which photoreceptors could be reliably quantified were obtained in 18 of 41 subjects,¹⁶ and of those 18, all had quantifiable data from at least 1 follow-up visit and 7 of these had quantifiable data from 2 follow-up visits (Table 2). In one subject (CEI-001), “baseline” data were those acquired during the second visit because of difficulty capturing quantifiable data at the first imaging session. In one subject (PCI-005), there were no quantifiable data obtained until the fourth overall visit, 26 months after the first imaging session (data not shown). For information regarding which visits yielded countable images for all subjects, see Table 1.

Cone density measurements revealed 2 groups of distinct cone density—one of higher density (greater than 25,000 cones/mm², 4 subjects) and a larger group (14 subjects) with lower density (Figure 3). Because of the large difference between the values in these groups, the lower density group was analyzed separately from the higher density group, which was too small for independent analysis. Linear modeling of the cone density values with a random subject intercept in the lower density group revealed no significant slope ($P = 0.126$), which indicated that these cone populations were stable throughout the follow-up period (Figure 4). The mean \pm SD percent change in cone density from baseline was $1 \pm 13\%$ (range -22 to $+23\%$) at the first (6-month) follow-up visit ($n = 14$) and $1 \pm 15\%$ (range -15 to $+21\%$) at the second (12-month) follow-up visit ($n = 6$). Qualitative assessment of these retinas over time indicates

that there is often no change in the cone mosaic (Figure 5).

For the 4 subjects with higher baseline cone density, their values at the first follow-up visit at which cone density could be measured changed by -22% (BPE-018), -16% (CEI-006), $+3\%$ (PCI-021), and 0% (UFC-004). These visits occurred at 7, 12, 7, and 7 months, respectively. Subject PCI-021 had a second

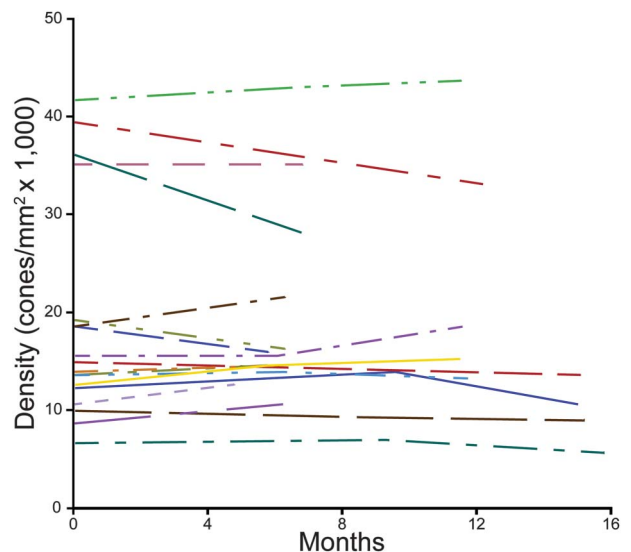


Fig. 3. Peak cone density values for 18 subjects for whom cone density was measured over the follow-up period. Note the 2 clusters of subjects, one group of 4 subjects with peak density greater than 25,000 cones/mm², and the remaining 14 subjects below that threshold. Subjects with densities lower than 25,000 cones/mm² showed no significant change in their peak cone density value ($P = 0.126$). The group of higher density subjects was too small for statistical analysis.

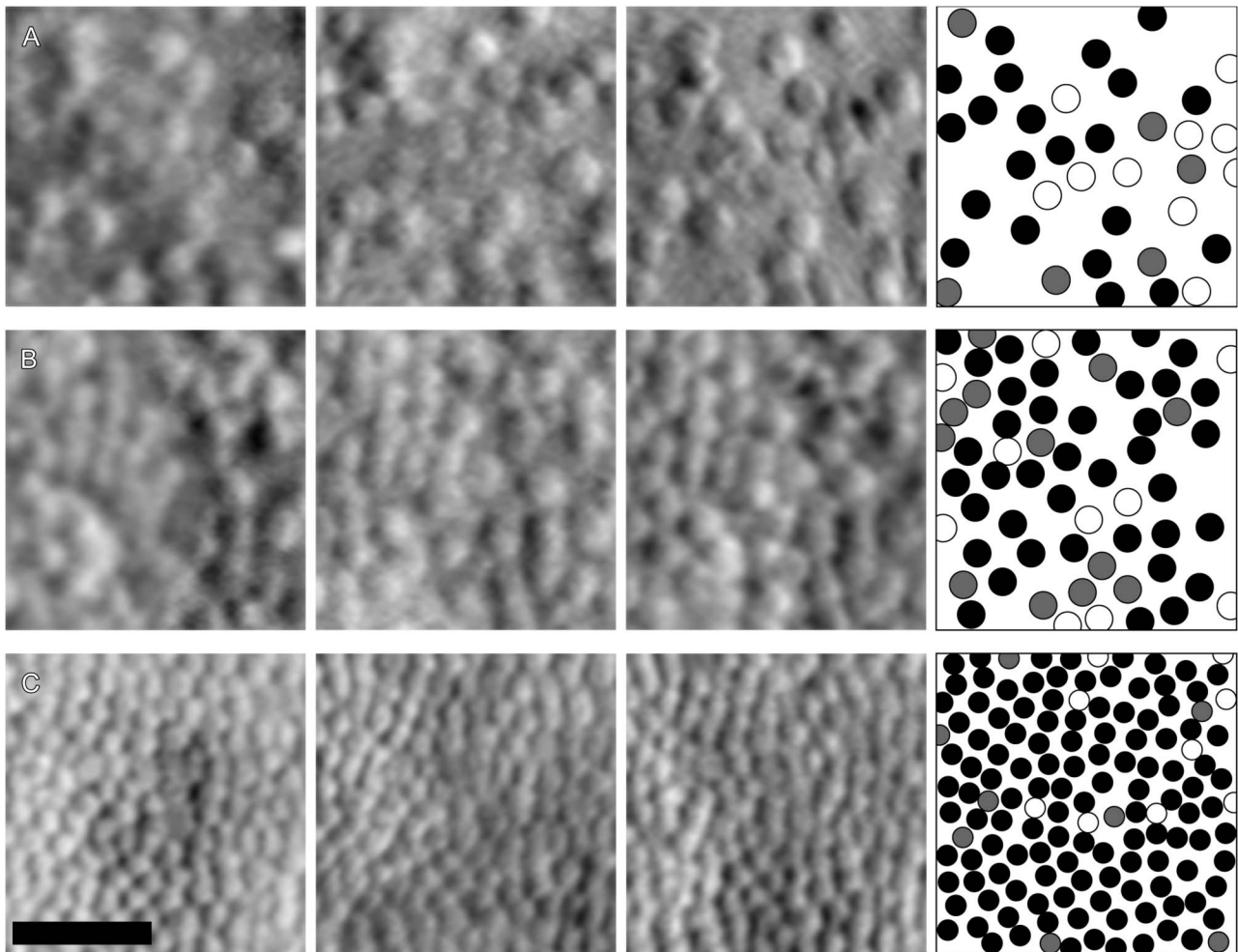


Fig. 4. Regions of interest that were counted at three time points in three subjects. Individual cone cells can be tracked across all three time points in these images. Although differences in image quality and distortion did cause some changes in the ability to identify cells, the same cones were present in all three images for each of these subjects. Shown in the right column are the cone locations coded by the number of time points the cell at that location was counted: white, 1 time point; gray, 2 time points; black, 3 time points. **A.** Subject BPE-003 had follow-up visits at 8 and 15 months from baseline. **B.** Subject PCI-017 had follow-up visits at 6 and 11 months from baseline. **C.** Subject PCI-021 had follow-up visits at 7 and 12 months from baseline. Scale = 25 μm .

follow-up visit, in which we observed a change in cone density of +5% compared with baseline. Table 2 provides cone density values from all visits.

Discussion

As with the previously reported baseline imaging,¹⁶ there was variability in the ability to quantify measurements of cone structure in these subjects with achromatopsia across the full follow-up period. Difficulty in obtaining images was most often due to nystagmus, which tends to decrease with age in achromatopsia.^{4,20} The reduced nystagmus with age resulted in improved image quality in subsequent visits for some younger subjects, notably subject PCI-005 whose images were not quantifiable at baseline (age = 11 years) but nystag-

mus was decreased sufficiently by 26 months after baseline (age = 13 years) to quantify foveal cone structure. Other reasons for image quality differences include eye dryness and subject fatigue, which often exacerbates nystagmus. These and similar factors prevented quantification of foveal cone structure in some subjects despite quantifiable images at a previous visit. This variability in image quality is an important, although not insurmountable, limiting factor in using AOSLO imaging to monitor cone structure over time. Strategies to mitigate the effects of eye movement on AOSLO imaging, such as high-speed eye tracking, should be developed to assist with imaging in this and similar patient populations to improve reliability of obtaining quantifiable images in longitudinal studies.

Foveal cone density seemed to be generally stable, although all of the subjects analyzed had relatively

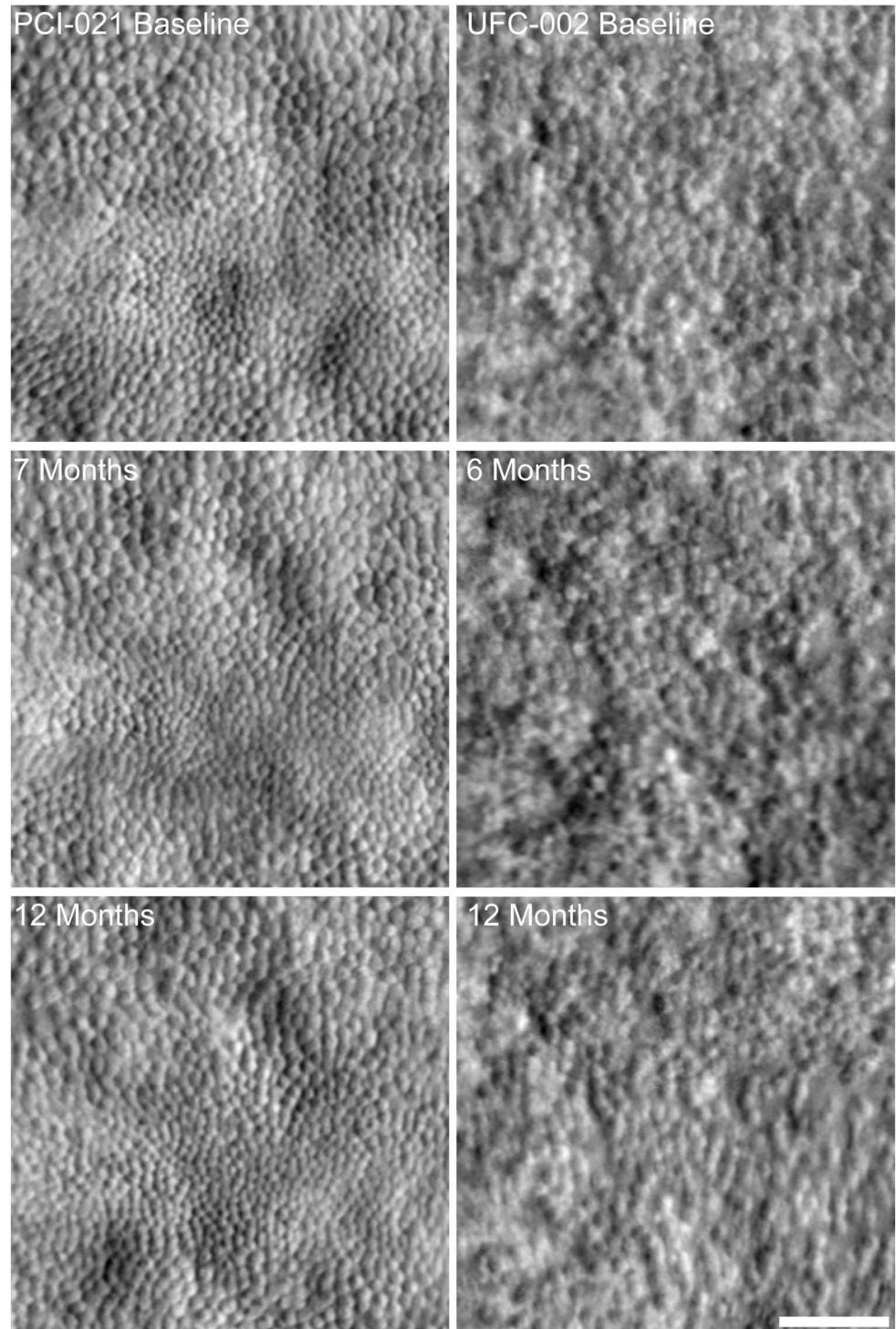


Fig. 5. A larger field image of the foveal cone mosaic of subjects PCI-021 and UFC-002. As seen in Figure 4, there is little to no change in the cone mosaic over a 12-month follow-up period for these subjects. Although there are slight differences in distortion and blurring throughout the images, there is no large-scale remodeling observed in the cone structure at the foveae of these subjects. Scale = 50 μm .

low baseline cone density values. Of the four subjects with markedly higher cone density (not included in the density modeling), two showed steep decreases in density whereas the other two had stable cone density. One possibility is that there is greater potential for cellular change in retinas with

a higher cone density; however, more subjects with relatively high cone density need to be followed longitudinally. It is important to note that our cone density measurements relied on manual identification of cone photoreceptors in the split-detector images. Subjective interpretation of structural

features in the image, as well as observer experience can impact the ability to consistently identify cellular features. This is an effect that we attempted to minimize using a single, experienced observer for all measurements—the result was highly repeatable measurements in our data. Not all observers may perform equally well, indeed previous work has shown poor interobserver reliability in estimates of cone density derived from manual analysis of split-detector images of the peripheral retina in achromatopsia.³⁶ As such, efforts should be made to ensure observers are well trained, and to automate³⁷ and standardize split-detector AOSLO cell detection in future studies.

Our OCT assessment showed a stable qualitative grading assessment for 34/41 subjects in this study; the number of subjects who showed an increased degree of disruption over time (5/41) was comparable to that previously observed (2/37) for a different group of subjects with achromatopsia.⁸ Another study observed qualitative outer retinal changes in five young subjects, but not the three older subjects studied.¹⁰ The changes that we observed primarily occurred in younger subjects (ages 11, 13, 15, 16, 17, 30, and 33). These results are in line with the observations of Thomas et al,¹⁰ who reported that the majority of changes were observed in the younger retinas. Additionally, Lee et al³⁸ reported that young children followed over a period of 5 months to 35 months exhibited increases and decreases in disruption, in some cases in the same eye, over the follow-up period. Not all of the younger subjects showed a change in our study, and the youngest subjects in fact had stable outer retinal appearance. Optical coherence tomography images in two subjects (CEI-009 and PCI-005) seemed to have less disrupted EZ (IS/OS) bands on follow-up. This finding is likely due to slight changes in the scan location at the fovea. Small degrees of disruption may be missed (or captured) depending on the exact scan location; displacement by only a few microns may affect the assessed grade of the EZ (IS/OS) band. This highlights the importance of scanning the identical retinal location over time, which often requires obtaining multiple images when dealing with patients with nystagmus.

Foveal ONL thickness increased very slightly in our subjects during the follow-up period. This result is not unprecedented, as ONL thickening has been previously observed with aging,³⁹ although it does contradict other similar measurements made in the achromatopsia retina that indicate either a stable or thinning ONL.^{8–10,40} The statistically significant change ($P = 0.02$) might not be generalizable to other

populations of subjects with achromatopsia. Furthermore, the measured change was very slight; with axial resolution of our OCT images of roughly $2.5 \mu\text{m}/\text{pixel}$, and at thickness rate of change of $0.184 \mu\text{m}/\text{month}$, a single-pixel thickness change would take over a year to be appreciable.

This study spanned a relatively short time frame—less than 2 years for most subjects. Thus, the stability observed may simply be due to a very slowly progressing nature in this condition, and perhaps additional follow-up in this cohort will reveal decreasing cone populations over a longer time course. Significantly, although achromatopsia is a very slowly progressing condition, our results hold promise for the development of gene therapy as there remains a cellular target present in these retinas for a very long period—supported by the presence of foveal cones in retinas over a wide age range. Indeed, only subjects with an atrophic foveal lesion lacked foveal cones, and no relationship between cone structure and age was observed in a previously reported cross-sectional analysis of this cohort.¹⁶ Having detectable cone structure may not be the only factor influencing a potential therapeutic window, but it is clearly a prerequisite for any gene therapeutic attempts.⁴¹ Taken together, our results suggest that OCT and AOSLO may be useful in monitoring structural changes after treatment.²⁶

Key words: achromatopsia, gene therapy, cone photoreceptor, color vision, imaging, adaptive optics, retinal degeneration.

Acknowledgments

The authors acknowledge Robert Cooper and Melissa Wilk for their contributions to this work.

The members of the ACHM-001 study group include: Applied Genetics Technologies Corporation: J. D. Chulay, June Lato, Rabia Ozden, and John Burnett. Bascom Palmer Eye Institute at University of Miami: B. L. Lam, Potyra Rosa, and Jennifer Verriotto. Casey Eye Institute at Oregon Health and Science University: M. E. Pennesi, P. Yang, R. G. Weleber, Mihir Wanchoo, and Deanna Ternes. Casey Eye Institute Reading Center: M. Parker, L. R. Erker, and D. J. Wilson. Casey Eye Institute Molecular Diagnostic Lab: John Chiang. The Chicago Light-house: G. A. Fishman, F. T. Collison, Carol White and Paola Andreuzzi. Medical College of Wisconsin: J. Carroll, A. Dubra, Vesper Williams, P. Summerfelt, E. J. Patterson and C. S. Langlo. University of Florida: W. W. Hauswirth. Vitreo Retinal Associates of Gainesville: C. N. Kay and J. Zhang.

References

- Kohl S, Zobor D, Chiang W, et al. Mutations in the unfolded protein response regulator *ATF6* cause the cone dysfunction disorder achromatopsia. *Nat Genet* 2015;47:757–765.
- Kohl S, Marx T, Giddings I, et al. Total colourblindness is caused by mutations in the gene encoding the alpha-subunit of the cone photoreceptor cGMP-gated cation channel. *Nat Genet* 1998;19:257–259.
- Kohl S, Baumann B, Rosenberg T, et al. Mutations in the cone photoreceptor G-protein α -subunit gene *GNAT2* in patients with achromatopsia. *Am J Hum Genet* 2002;71:422–425.
- Kohl S, Varsanyi B, Antunes GA, et al. *CNGB3* mutations account for 50% of all cases with autosomal recessive achromatopsia. *Eur J Hum Genet* 2005;13:302–308.
- Thiadens AA, Slingerland NW, Roosing S, et al. Genetic etiology and clinical consequences of complete and incomplete achromatopsia. *Ophthalmology* 2009;116:1984–1989.
- Zobor D, Zobor G, Kohl S. Achromatopsia: on the doorstep of a possible therapy. *Ophthalmic Res* 2015;54:103–108.
- Sundaram V, Wilde C, Aboshiha J, et al. Retinal structure and function in achromatopsia: implications for gene therapy. *Ophthalmology* 2014;121:234–245.
- Aboshiha J, Dubis AM, Cowing J, et al. A prospective longitudinal study of retinal structure and function in achromatopsia. *Invest Ophthalmol Vis Sci* 2014;55:5733–5743.
- Thiadens AA, Somervuo V, van den Born LI, et al. Progressive loss of cones in achromatopsia: an imaging study using spectral-domain optical coherence tomography. *Invest Ophthalmol Vis Sci* 2010;51:5952–5957.
- Thomas MG, McLean RJ, Kohl S, et al. Early signs of longitudinal progressive cone photoreceptor degeneration in achromatopsia. *Br J Ophthalmol* 2012;96:1232–1236.
- Warren C, Scoles DH, Dubis A, et al. Imaging cone structure in autosomal dominant cone rod dystrophy caused by *GUCY2D* mutations. *Invest Ophthalmol Vis Sci* 2014;55:1102.
- Genead MA, Fishman GA, Rha J, et al. Photoreceptor structure and function in patients with congenital achromatopsia. *Invest Ophthalmol Vis Sci* 2011;52:7298–7308.
- Merino D, Duncan JL, Tiruveedhula P, Roorda A. Observation of cone and rod photoreceptors in normal subjects and patients using a new generation adaptive optics scanning laser ophthalmoscope. *Biomed Opt Express* 2011;2:2189–2201.
- Dubis AM, Cooper RF, Aboshiha J, et al. Genotype-dependent variability in residual cone structure in achromatopsia: towards developing metrics for assessing cone health. *Invest Ophthalmol Vis Sci* 2014;55:7303–7311.
- Wilk MA, McAllister JT, Cooper RF, et al. Relationship between foveal cone specialization and pit morphology in albinism. *Invest Ophthalmol Vis Sci* 2014;55:4186–4198.
- Langlo CS, Patterson EJ, Higgins BP, et al. Residual foveal cone structure in *CNGB3*-associated achromatopsia. *Invest Ophthalmol Vis Sci* 2016;57:3984–3995.
- Zhang T, Godara P, Blancob ER, et al. Variability in human cone topography assessed by adaptive optics scanning laser ophthalmoscopy. *Am J Ophthalmol* 2015;160:290–300.
- Curcio CA, Sloan KR, Kalina RE, Hendrickson AE. Human photoreceptor topography. *J Comp Neurol* 1990;292:497–523.
- Michaelides M, Hunt DM, Moore AT. The cone dysfunction syndromes. *Br J Ophthalmol* 2004;88:291–297.
- Simunovic MP, Moore AT. The cone dystrophies. *Eye* 1998;12:553–565.
- Yang P, Michaels KV, Courtney RJ, et al. Retinal morphology of patients with achromatopsia during early childhood: implications for gene therapy. *JAMA Ophthalmol* 2014;132:823–831.
- Roorda A. Applications of adaptive optics scanning laser ophthalmoscopy. *Optom Vis Sci* 2010;87:260–268.
- Roorda A, Duncan JL. Adaptive optics ophthalmoscopy. *Annu Rev Vis Sci* 2015;1:19–50.
- Flatter JA, Cooper RF, Dubow MJ, et al. Outer retinal structure after closed-globe blunt ocular trauma. *Retina* 2014;34:2133–2146.
- Sun LW, Johnson RD, Langlo CS, et al. Assessing photoreceptor structure in retinitis pigmentosa and Usher syndrome. *Invest Ophthalmol Vis Sci* 2016;57:2428–2442.
- Talcott KE, Ratnam K, Sundquist S, et al. Longitudinal study of cone photoreceptors during retinal degeneration and in response to ciliary neurotrophic factor treatment. *Invest Ophthalmol Vis Sci* 2011;52:2219–2226.
- Wang Q, Tuten WS, Lujan BJ, et al. Adaptive optics microperimetry and OCT images show preserved function and recovery of cone visibility in macular telangiectasia type 2 retinal lesions. *Invest Ophthalmol Vis Sci* 2015;56:778–786.
- Horton JC, Parker AB, Botelho JV, Duncan JL. Spontaneous regeneration of human photoreceptor outer segments. *Sci Rep* 2015;5:12364.
- Dubra A, Sulai Y. Reflective afocal broadband adaptive optics scanning ophthalmoscope. *Biomed Opt Express* 2011;2:1757–1768.
- Scoles D, Sulai YN, Langlo CS, et al. In vivo imaging of human cone photoreceptor inner segments. *Invest Ophthalmol Vis Sci* 2014;55:4244–4251.
- Dubra A, Harvey Z. Registration of 2D images from fast scanning ophthalmic instruments. In: Fischer B, Dawant B, Lorenz C, eds. *Biomed Image Registration*. Berlin, Germany: Springer-Verlag; 2010:60–71.
- Schindelin J, Arganda-Carreras I, Frise E, et al. Fiji: an open-source platform for biological-image analysis. *Nat Methods* 2012;9:676–682.
- Arganda-Carreras I, Sorzano COS, Marabini R, et al. Consistent and elastic registration of histological sections using vector-spline regularization. In: Beichel RR, Sonka M, eds. *Computer Vision Approaches to Medical Image Analysis*. Berlin, Germany: Springer; 2006:85–95.
- Garrioch R, Langlo C, Dubis AM, et al. Repeatability of in vivo parafoveal cone density and spacing measurements. *Optom Vis Sci* 2012;89:632–643.
- Liu BS, Tarima S, Vistocky A, et al. The reliability of parafoveal cone density measurements. *Br J Ophthalmol* 2014;98:1126–1131.
- Abozaid MA, Langlo CS, Dubis AM, et al. Reliability and repeatability of cone density measurements in patients with congenital achromatopsia. *Adv Exp Med Biol* 2016;854:277–283.
- Cunefare D, Cooper RF, Higgins B, et al. Automatic detection of cone photoreceptors in split detector adaptive optics scanning light ophthalmoscope images. *Biomed Opt Express* 2016;7:2036–2050.
- Lee H, Purohit R, Sheth V, et al. Retinal development in infants and young children with achromatopsia. *Ophthalmology* 2015;122:2145–2147.
- Chui TY, Song H, Clark CA, et al. Cone photoreceptor packing density and the outer nuclear layer thickness in healthy subjects. *Invest Ophthalmol Vis Sci* 2012;53:3545–3553.
- Thomas MG, Kumar A, Kohl S, et al. High-resolution in vivo imaging in achromatopsia. *Ophthalmology* 2011;118:882–887.
- Jacobson SG, Aleman TS, Cideciyan AV, et al. Identifying photoreceptors in blind eyes caused by *RPE65* mutations: prerequisite for human gene therapy success. *Proc Natl Acad Sci U S A* 2005;102:6177–6182.